Electronic and magnetic properties of $BiFeO_3$ with intrinsic defects: First-principles prediction*

Yang Rui-Peng(杨瑞鹏)[a], Lin Si-Xian(林思贤)[a], Fang Xiao-Gong(方潇功)[a], Qin Ming-Hui(秦明辉)[a], Gao Xing-Sen(高兴森)[a], Zeng Min(曾 敏)[a]†, and Liu Jun-Ming(刘俊明)[b]

[a] *Institute for Advanced Materials, South China Normal University, Guangzhou* 510006, *China*
[b] *Laboratory of Solid State Microstructures, Nanjing University, Nanjing* 210093, *China*

(Received 31 October 2013; revised manuscript received 3 December 2013; published online 10 April 2014)

The electronic structure, magnetism, and dielectric functions of $BiFeO_3$ with intrinsic vacancies, including Bi-, Fe-, and O-vacancies (denoted as V_{Fe}, V_{Bi}, and V_O, respectively) are investigated using the first-principles density functional theory plus U calculations. It is revealed that the structural distortions associated with those vacancies impose significant influences on the total density of state and magnetic behaviors. The existence of V_{Bi} favors the excitation of the O_{2p} state into the band gap at 0.4 eV, while the O_{2p} and Fe_{3d} orbitals are co-excited into the band gap around 0.45 eV in V_{Fe}. Consequently, a giant net magnetic moment of 1.96 μ_B is generated in V_{Fe}, and a relatively small moment of 0.13 μ_B is induced in V_{Bi}, whereas V_O seems magnetically inactive. The giant magnetic moment generated in V_{Fe} originates from the suppression of the spatially modulated antiferromagnetic spin structure. Furthermore, V_{Fe} and V_{Bi} have strong influences on dielectric function, and induce some strong peaks to occur in the lower energy level. In contrast, V_O has a small effect.

Keywords: $BiFeO_3$, vacancies, magnetization, dielectric functions

PACS: 71.20.–b, 71.55.–i, 77.22.–d, 75.10.–b **DOI:** 10.1088/1674-1056/23/6/067102

1. Introduction

Recently, enormous attention has been paid to multiferroic materials that process ferroelectric (FE) and magnetic properties simultaneously, which offers extra degrees of freedom so that electric polarization can be switched by a magnetic field and magnetization can be adjusted by an electric field. The mutual control of electric and magnetic properties can manifest itself as the magnetoelectric effect, which is of significant interest for applications in microelectronics, storage memory, and sensor techniques.[1,2] Single-phase $BiFeO_3$ (BFO) exhibiting antiferromagnetic (AFM) order with Neel point $T_N \sim 625$ K and FE Curie point $T_C \sim 1083$ K is famous for its room temperature multiferroicity.[3–11] Although, large spontaneous polarization $P \sim 100$ $\mu C/cm^2$ has been reported in thin film and single crystal forms, the ferromagnetism is weak due to its AFM order. Consequently, the coupling between ferroelectric and ferromagnetic orders is very weak so that its practical applications are limited greatly. In the past few decades, many methods have been attempted to enhance the magnetism along with the coupling properties. Among them, the substitution of A- and/or B-sites by other elements in BFO has been extensively adopted with the aim to suppress the spatial-modulated AFM spin ordering. For instance, Yuan *et al.*[12] and Gu *et al.*[13] reported on the enhanced ferromagnetism in BFO ceramics through the substitution of Bi^{3+} by Nd^{3+}, and Fe^{3+} by Ti^{4+} ions, respectively. However, doping may sometimes introduce some impurity phases and/or induce structural transitions so that the intrinsic multiferroic properties in perfect BFO can be deteriorated.

Alternatively, the intrinsic lattice defects in BFO, including cation and anion vacancies, have been proposed to serve as a possible source of magnetization. Theoretically, Ederer and Spaldin[14] reported on a slightly improved magnetization in BFO by inducting oxygen vacancies. The effects of oxygen vacancies on the electronic structures and/or optical responses were addressed by Ju and Cai[15] and Lou *et al.*[16] The mechanism of formation energy in intrinsic vacancies BFO was dealt with too.[17,18] Actually, the lattice vacancies in BFO can be artificially introduced by nonstoichiometric compositions and preparation processing. In particular, Fe vacancies have a direct effect on spin ordering, implying that the magnetism of BFO will be more or less changed by these vacancies. Furthermore, some relevant properties, such as electronic structure and dielectric susceptibility, are also sensitive to these defects. Thus, a detailed study on the role of defects in BFO, in particular, the response of magnetism and dielectric susceptibility, is desired. In this paper, we investigate comprehensively the effects of three possible types of vacancies on the electronic structure, magnetism, and dielectric function of BFO by using the spin-polarized density functional theory calculations. The results reveal that V_{Bi} and V_{Fe} generate net magnetizations of ~ 0.13 μ_B and 1.96 μ_B per vacancy, respectively, while V_O seems magnetically inactive. In contrast to V_O, V_{Fe} and V_{Bi}

*Project supported by the National Natural Science Foundation of China (Grant Nos. 51101063, 51072061, and 51172067) and the Natural Science Foundation of Guangdong Province, China (Grant No. S2011040003205).

†Corresponding author. E-mail: zengmin@scnu.edu.cn

© 2014 Chinese Physical Society and IOP Publishing Ltd

have larger influences on dielectric function.

2. Computation method

Our first-principles calculations were performed using the projector augmented wave (PAW) method with the local spin-density approximation plus the on-site repulsion (LSDA + U)[19,20] as implemented in the Vienna *ab initio* simulation package (VASP).[21,22] We used $U_{\rm eff} = 3$ eV on Fe 3d states for a better description of the localized transition, and it provides a reasonable magnetic structure.[18] We treated the basis with Bi $5d^{10}6s^26p^3$, Fe $3p^63d^64s^2$, and O $2s^22p^4$. The energy cutoff of 400 eV was used for the plane wave expansion of the PAW, and the tetrahedron method was adopted for the Brillouin-zone integrations. To model bulk BFO with single crystal form under various vacancy conditions, we build a 2×2×2 periodic supercell (80 atoms) based on the optimized primitive cell. A vacancy is created by removing one atom in the supercell, which corresponds to a defect concentration of 6.25% for Bi vacancy (denoted as $V_{\rm Bi}$) and Fe vacancy (denoted as $V_{\rm Fe}$), and 2.08% for the O vacancy (denoted as $V_{\rm O}$). The crystal structure of the BFO supercell is shown in Fig. 1. Consider the fact that the fully relaxed crystal structure [$a = 5.56$ Å, $\alpha = 59.75°$] with primitive cell in perfect BFO structure shows an $R3c$ rhombohedral symmetry, which is in good agreement with the experimental values [$a = 5.63$ Å, $\alpha = 59.35°$],[23] that is to say, the positions in each type of atom are equivalent so that an individual point defect can be created by removing randomly one atom in each type (see Fig. 1). After establishing three types of vacancies, their crystal structures for the equilibrium position of all the other atoms are relaxed in a 3×3×3 Monkhorst Pack grid of k points until the atomic forces are less than 1 meV/Å.

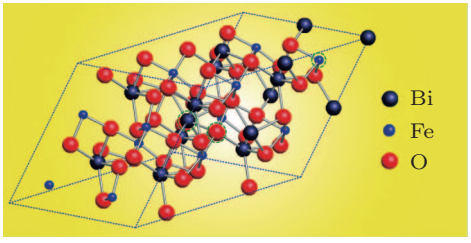


Fig. 1. (color online) Crystal structure of perfect BFO with the supercell (2×2×2). Vacancy configuration corresponds to the removal of one atom (with dotted circle) in each type. The black ball is Bi, the blue ball is Fe, and the red ball is O.

It is well known that the dielectric function is mainly attributed to electronic inter-band transitions. The imaginary part $\varepsilon_2(\omega)$ of the dielectric function is calculated from the momentum matrix elements between the occupied and unoccupied wave functions and given by the Fermi golden rule, i.e.,[24]

$$\varepsilon_2(\omega) = \frac{4\pi^2}{\Omega\omega^2} \sum_{i\in VB, j\in CB} \sum_k w_k |p^a_{ji}|^2 \delta(\varepsilon_{k_j} - \varepsilon_{k_i} - \omega), \quad (1)$$

where Ω is the unit-cell volume and ω is the photon energy, CB and VB denote the conduction and valence bands, respectively, and p^a_{ij} are the dipolar transition matrix elements and $p^a_{ij} = \langle k_j|P_a|k_i\rangle$ that are obtained from the self-consistent band structures within the PAW formalism. Here, $|k_n\rangle$ is the n-th Bloch state wave function with crystal momentum k, and a denotes the Cartensian component. The real part $\varepsilon_1(\omega)$ of the dielectric function is evaluated from imaginary part $\varepsilon_2(\omega)$ by the Kramers–Kronig transformation

$$\varepsilon_1(\omega) = 1 + \frac{2}{\pi} P \int_0^\infty \mathrm{d}\omega \frac{\omega'\varepsilon_2(\omega')}{\omega'^2 - \omega^2},$$

in which P is the principle value of the integral.

3. Results and discussion

The calculated net magnetic moments of BFO with three types of vacancies as well as perfect BFO are listed in Table 1. It is found that the structural distortions in the vacancy systems exert great influences on the magnetic moments, and the values in defects are significantly different from that of perfect BFO. Compared with the case with no magnetic moment in perfect BFO, $V_{\rm Fe}$ and $V_{\rm Bi}$ vacancies induce magnetic moments of 1.96 $\mu_{\rm B}$ and 0.13 $\mu_{\rm B}$, respectively, while the induced magnetic moment is small in $V_{\rm O}$. Using the calculated results, we evaluate the magnetic moments to be ∼ 18.38, 1.22, and 0.29 emμ/g for $V_{\rm Fe}$, $V_{\rm Bi}$, and $V_{\rm O}$, respectively (1 $\mu_{\rm B}$ per unit cell corresponds to ∼ 150 emμ/g). Experimentally, there is still a lot of debate on the magnetic properties of BFO. Wang *et al.*[25] reported on a 0.5 $\mu_{\rm B}$/Fe in an epitaxial BFO thin film and proposed that the large value is due to the coupling between magnetic dipoles and the strain arising from a lattice-mismatched substrate, Meanwhile other measurements yielded a magnetic moment being two orders of magnitude smaller, and it is argued that the substantial magnetization could be defect-relevant.[26] By contrast, bulk BFO samples fabricated using various techniques do not exhibit substantial magnetizations.[7,10] Furthermore, the two-point defects in Fe vacancy system (defect concentration up to 12.5%) with six different spin ordering configurations are calculated. The results reveal that the Fe vacancies prefer to occupy the ferromagnetically aligned planes from the energy viewpoint, and that the net magnetic moment is up to 8.3 $\mu_{\rm B}$. We also find that two point defects lying in two antiferromagnetically aligned planes produce no net magnetic moment. It must be mentioned that the total energy difference between the two kinds of spin structures is very small (20 meV) so that the giant moment generated in Fe vacancies needs a special spin ordering structure. This may be the reason that different magnetic moments were reported between ceramic and film forms.

Table 1. Calculated and evaluated magnetic moments of BFO with and without vacancies.

Structure	Perfect BFO	V_{Bi}	V_{Fe}	V_O
Defect concentration/%	0	6.25	6.25	2.08
Calculated magnetic moment/(μ_B/vacancy)	0	0.13	1.96	0.031
Evaluated magnetic moment/(emμ/g)	0	1.22	18.38	0.29

To clarify the origin of the magnetism induced by the lattice vacancies in BFO, we investigate the electronic structures of three types of vacancy systems via the density of states (DOS), and the results are shown in Fig. 2 along with the result of the perfect BFO for a comparison. For the perfect BFO (see Fig. 2(a)), our calculated band gap is about 2.4 eV, which is in good agreement with the previous experimental value (2.5 eV) and other theoretical results (2.2 eV$\sim$ 2.8 eV).[27–29] It is noticed that no magnetic moment occurring in the perfect BFO can be verified by the highly symmetrical DOS, while the significant DOS differences are present in the lattice vacancies BFO because of the broken symmetry of the original $R3c$ structure. For V_{Bi} (see Fig. 2(b)), a set of impure levels above VB can be found either in the majority DOS or minority DOS (see the dotted cycle), meaning a p-type conductive property, which is consistent with the experimental result.[30] The most interesting feature is that some in-gap electric states are found in the majority DOS, but not in the minority DOS, which induces a net magnetic moment. In addition, the in-gap electronic states at 0.4 eV originate mainly from the O_{2p} orbitals of the nearest O atom around the Bi vacancy (see Fig. 3(a)). Like the case of the perfect BFO, no electron is found at the Fermi level in V_{Fe}, and only in-gap electrons are found in the majority DOS. Oppositely, the minority DOS presents a clear shifting towards the left level so that this relatively large non-symmetrical DOS generates a large magnetic moment. From the partial DOS analysis it follows that the O_{2p} and Fe_{3d} orbitals near the Fe vacancy contribute to the in-gap electronic states around 0.45 eV (see Fig. 3(b)), implying that the strong Fe–O hybridization is responsible for the large magnetic moment. In contrast, V_O has a slight effect on the symmetry of DOS, but the band gap is significantly reduced, which is consistent with the other calculated one.[15]

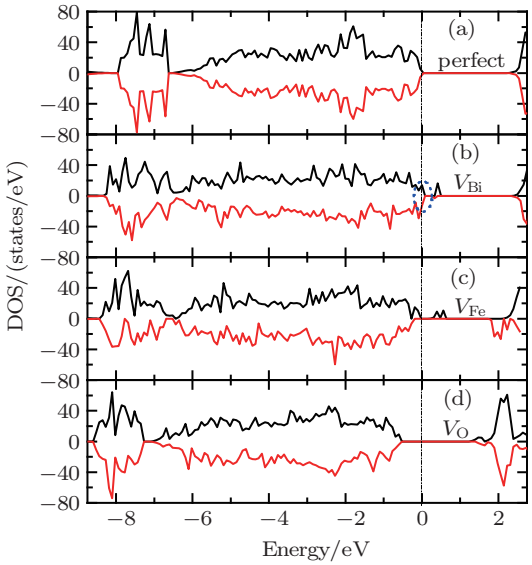


Fig. 2. (color online) Total DOSs of (a) the perfect BFO, (b) V_{Bi}, (c) V_{Fe}, and (d) V_O. The positive (negative) values represent the majority (minority). The zero-point energy is the Fermi level.

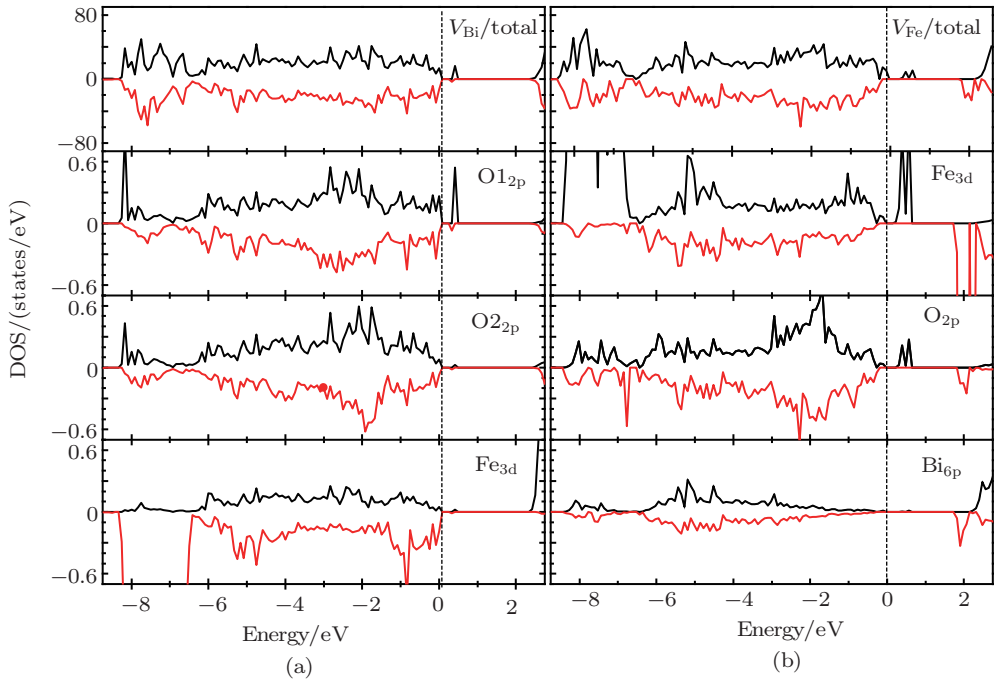


Fig. 3. (color online) Total and partial DOSs of (a) V_{Bi} and (b) V_{Fe}. The positive (negative) values represent the majority (minority), respectively. The zero-point energy is the Fermi level.

Figure 4 shows the charge density distributions of three types of vacancies and perfect BFO projected in the $(1\bar{1}0)$ plane. The horizontal axis is along the [110] direction and the vertical axis is along the [001] direction. For perfect structure (see Fig. 4(a)), the iso-charge lines are located at the center of each atom without any hybridization to some extent. For V_{Bi} (see Fig. 4(b)), the Bi vacancy (see the dotted cycle), corresponding to the center of negative charges, induces Coulomb repulse and attraction with the neighboring O and Fe atoms, respectively. Consequently, a significant distortion is observed in the FeO_6 octahedrons around the Bi vacancy, and makes a set of three Fe–O bond lengths slightly shortened from 1.9755 Å to 1.9293 Å so that a clear charge hybridization is present along the [001] direction. Also, the Fe vacancy makes the neighboring Bi and O atoms move inward and outward, respectively (see Fig. 4(c)). The FeO_6 octahedron is distorted significantly as the Fe atom has the most valence electrons, so that the bond length between the O and the Fe atoms is greatly shortened to 1.8780 Å along the [111] direction and the strong hybridizations occur between the O atoms and the Fe/Bi atoms. In contrast, for V_O (see Fig. 4(d)), all the cations near the O vacancy are slightly expanded outward and the shapes of charge density distributions do not change.

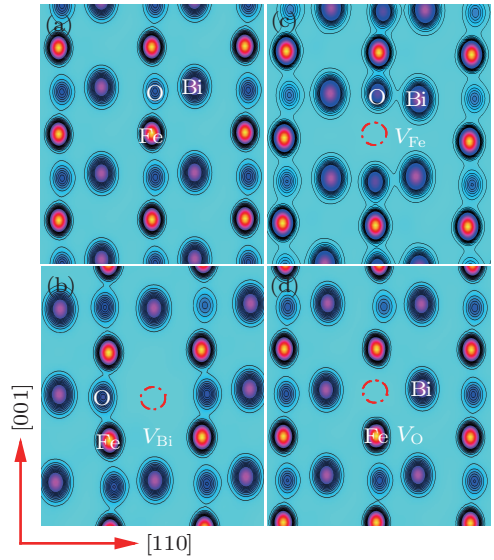


Fig. 4. (color online) Charge density distributions of (a) perfect BFO, (b) V_{Bi}, (c) V_{Fe}, and (d) V_O in the $(1\bar{1}0)$ plane. These vacancies are labeled by dotted circles separately.

In order to illustrate the origins of net magnetic moments of BFO with three types of vacancies, the magnetic moments of Fe atoms have been investigated as the magnetism in the BFO system is generated mainly by Fe atoms. For perfect structure, the magnetic moment of the Fe atom is about $\pm 4.159\ \mu_B$, whereas this system does not exhibit a net magnetic moment due to the Fe^{3+}–O–Fe^{3+} AFM spin ordering. Once a vacancy is introduced, the AFM spin ordering network is more or less disrupted, and/or the magnetic moments of the Fe atoms are changed. The largest magnetic moment of $1.96\ \mu_B$ in V_{Fe} is mainly attributed to the transition of spin ordering from antiferromagnetism to ferrimagnetism. It is noted that the value is not simply equal to the magnetic moment of an individual Fe atom. The reason is attributed to the fact that partial Fe^{3+} ions are changed into Fe^{2+} ions due to the charge compensatory mechanism (the magnetic moments of Fe^{2+} ions are $\pm 3.551\ \mu_B$). For V_{Bi} and V_O, although the spin structures still keep AFM spin orderings, the local magnetic moments of Fe atoms around their vacancies are reduced. From Fig. 4(b) it is found that the Bi vacancy induces a nonsymmetrical ion displacement of Fe atoms along the [010] direction so that the changes of magnetic moments of Fe atoms are different: one is $-3.551\ \mu_B$ and the other is $3.589\ \mu_B$. Thus, a small net magnetic moment of $0.13\ \mu_B$ is generated in V_{Bi}. In contrast, the effect of V_O on the net magnetic moment is negligible, and the key factor is that the change of magnetic moment of Fe atoms is almost symmetrical.

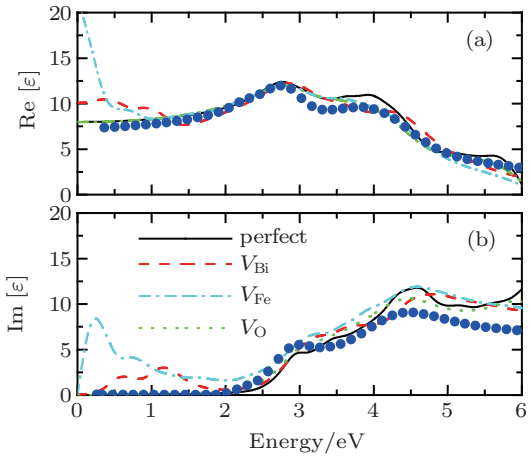


Fig. 5. (color online) Calculated dielectric functions of BFO with and without vacancies. (a) Real part and (b) imaginary part. Experimental data (solid circles) are cited from Ref. [31].

Finally, the calculated dielectric functions of BFO with and without vacancies are shown in Fig. 5 along with a comparison with experiment data.[31] Here, the theoretical dielectric function, ε, is defined as $\varepsilon = (\varepsilon_{xx} + \varepsilon_{yy} + \varepsilon_{zz})/3$ for $R3c$ symmetry. It is clear that the presence of V_O does not change the location of the main absorption peaks in comparison with those in perfect structure and experiment, which is consistent with the results reported by Ju *et al.*[15] in the relatively low oxygen concentration. The reason may be that the oxygen vacancies are always produced in the experimental process.[31] However, a significant discrepancy is found in the V_{Fe} and V_{Bi}, where some strong peaks appear at the lower energy level. As a matter of fact, the imaginary part $\varepsilon_2(\omega)$ of the dielectric function is directly related to the energy band structure. The peaks at 0.60 eV and 1.16 eV in V_{Bi} correspond mainly to the transitions of O 2p from VB to the excited lower-energy CB (see Fig. 3(a)). While the peaks at 0.24 eV and 0.75 eV in V_{Fe}

come mainly from the transitions of O 2p and Fe 3d from VB to the excited lower-energy CB (see Fig. 3(b)). Therefore, it can be concluded that V_{Fe} and V_{Bi} have strong influences on the dielectric function. In experiment, the dielectric response in BFO is influenced greatly due to the occurrance of volatilizing Bi ions and valence changing Fe ions.

4. Conclusions

In this paper, first-principles calculations are performed to investigate the electronic structures, magnetisms, and dielectric functions of BFO with three types of vacancies. The Fe and Bi vacancies induce net magnetic moments with the values of 1.96 μ_B and 0.13 μ_B, respectively. It is proposed that the induced net magnetic moments occur due to the suppression of the spatially modulated AFM spin structure and asymmetrical local magnetic moments of Fe atoms. However, the O vacancy has a slight effect on the net magnetic moment. Furthermore, V_{Fe} and V_{Bi} induce some strong peaks of dielectric functions to form at the lower energy level, while the effect of V_O on electric functions is small. The enhanced magnetism in Fe- and/or Bi-deficient BFO predicts a possible improvement in coupling between ferromagnetic and ferroelectric orderings, which opens the way for improving the multiferroic properties in prototypical BFO materials.

References

[1] Smolenskiĭ G and Chupis I 1982 *Sov. Phys. Usp.* **25** 475
[2] Wang K F, Liu J M, and Ren Z F 2009 *Adv. Phys.* **58** 321
[3] Wang J, Neaton J, Zheng H, Nagarajan V, Ogale S, Liu B, Viehland D, Vaithyanathan V, Schlom D and Waghmare U 2003 *Science* **299** 1719
[4] Catalan G and Scott J F 2009 *Adv. Mater.* **21** 2463
[5] Zhang S T, Zhang Y, Lu M H, Du C L, Chen Y F, Liu Z G, Zhu Y Y, Ming N B and PanX Q 2006 *Appl. Phys. Lett.* **88** 162901
[6] Lisenkov S, Kornev I A and Bellaiche L 2009 *Phys. Rev. B* **79** 012101
[7] Selbach S M, Einarsrud M A, Tybell T and Grande T 2007 *J. Am. Ceram. Soc.* **90** 3430
[8] Hu Z Q, Li M Y, Yu Y, Liu J, Pei L, Wang J, Liu X L, Yu B F and Zhao X Z 2010 *Solid State Commun.* **150** 1088
[9] Prosandeev S, Kornev I A and BellaicheL 2011 *Phys. Rev. B* **83** 020102(R)
[10] Huang F, Lu X, Wang Z, Lin W, Kan Y, Bo H, Cai W and Zhu J 2009 *Appl. Phys. A* **97** 699
[11] Fischer P, Polomska M, Sosnowska I and Szymanski M 1980 *J. Phys. C: Solid State Phys.* **13** 1931
[12] Yuan G L, Or S W, Liu J M and Liu Z G 2006 *Appl. Phys. Lett.* **89** 052905
[13] Gu Y H, Wang Y, Chen F, Chan H W and Chen W P 2010 *J. Appl. Phys.* **108** 094112
[14] Ederer C and Spaldin N A 2005 *Phys. Rev. B* **71** 224103
[15] Ju S and Cai T Y 2009 *Appl. Phys. Lett.* **95** 231906
[16] Lou Y H, Song G L, Chang F G and Wang Z K 2010 *Chin. Phys. B* **19** 077702
[17] Zhang Z, Wu P, Chen L and Wang J 2010 *Appl. Phys. Lett.* **96** 232906
[18] Paudel T R, Jaswal S S and Tsymbal E Y 2012 *Phys. Rev. B* **85** 104409
[19] Blöchl P E 1994 *Phys. Rev. B* **50** 17953
[20] Anisimov V I, Aryasetiawan F and Lichtenstein A 1997 *J. Phys.: Condens. Matter* **9** 767
[21] Kresse G and Hafner J 1993 *Phys. Rev. B* **47** 558
[22] Kresse G and Furthnuller J 1996 *Phys. Rev. B* **54** 11169
[23] Kubel F and Schmid H 1990 *Acta Crystallogr. Sect. B: Struct. Sci.* **46** 698
[24] Zeng M, Or S W and Chan W H L 2010 *J. Appl. Phys.* **107** 043513
[25] Wang J, Neaton J B, Zheng H, Nagarajan V, Ogale S B, Liu B, Viehland D, Vaithyanathan V, Schlom D G, Waghmare U V, Spaldin N A, Rabe K M, Wuttig M and Ramesh R 2003 *Science* **299** 1719
[26] Shimada T, Uratani Y and Kitamura T 2012 *Appl. Phys. Lett.* **100** 162901
[27] Clark S and Robertson J 2007 *Appl. Phys. Lett.* **90** 132903
[28] Kanai T, Ohkoshi S and Hashimoto K 2003 *J. Phys. Chem. Solids* **64** 391
[29] Gao F, Yuan Y, Wang K, Chen X, Chen F, Liu J M and Ren Z 2006 *Appl. Phys. Lett.* **89** 102506
[30] Kim T H, Jeon B C, Min T, Yang S M, Lee D, Kim Y S, Baek S H, Saenrang W, Eom C B and Song T K 2012 *Adv. Funct. Mater.* **22** 4962
[31] Ihlefeld J, Podraza N, Liu Z, Rai R, Xu X, Heeg T, Chen Y, Li J, Collins R and Musfeldt J 2008 *Appl. Phys. Lett.* **92** 142908